



Published in final edited form as:

Nat Cell Biol. 2002 July ; 4(7): 509–513. doi:10.1038/ncb811.

A PtdInsP₃- and Rho GTPase-mediated positive feedback loop regulates neutrophil polarity

Orion D. Weiner^{*,†}, Paul O. Nielsen[‡], Glenn D. Prestwich[§], Marc W. Kirschner^{*}, Lewis C. Cantley[†], and Henry R. Bourne^{¶, #}

^{*}Department of Cell Biology, Harvard Medical School, 240 Longwood Ave/ C-1, Boston, MA 02115, USA

[†]Department of Cell Biology, Harvard Medical School, Division of Signal Transduction, Beth Israel Deaconess Medical Center, Boston, MA 02115, USA

[‡]Echelon Research Laboratories, 420 Chipeta Way, Suite 180, Salt Lake City, UT 84108

[§]Department of Medicinal Chemistry, University of Utah, 419 Wakara Way, Suite 205, Salt Lake City, UT 84108, USA

[¶]Department of Cellular and Molecular Pharmacology, University of California, San Francisco, CA 94143-0450, USA

Abstract

When presented with a gradient of chemoattractant, many eukaryotic cells respond with polarized accumulation of the phospholipid PtdIns(3,4,5)P₃. This lipid asymmetry is one of the earliest readouts of polarity in neutrophils, *Dictyostelium discoideum* and fibroblasts. However, the mechanisms that regulate PtdInsP₃ polarization are not well understood. Using a cationic lipid shuttling system, we have delivered exogenous PtdInsP₃ to neutrophils. Exogenous PtdInsP₃ elicits accumulation of endogenous PtdInsP₃ in a positive feedback loop that requires endogenous phosphatidylinositol-3-OH kinases (PI(3)Ks) and Rho family GTPases. This feedback loop is important for establishing PtdInsP₃ polarity in response to both chemoattractant and to exogenous PtdInsP₃; it may function through a self-organizing pattern formation system. Emergent properties of positive and negative regulatory links between PtdInsP₃ and Rho family GTPases may constitute a broadly conserved module for the establishment of cell polarity during eukaryotic chemotaxis.

By combining genetics and pharmacology to inhibit signalling cascades, we are beginning to understand the components that are necessary for directed cell polarity. However, the mechanisms through which these components interact to produce cell polarity are less well understood. Here, we focus on the role of the phospholipid PtdInsP₃ in the cell polarization process. This lipid has a strong polarity during chemotaxis of *Dictyostelium*^{1,2}, neutrophils³ and fibroblasts⁴. The internal gradient of PtdInsP₃ exceeds that of the external chemoattractant gradient and is one of the most upstream signalling molecules known to do so during cell polarization³. Pharmacological, biochemical and genetic inhibition of

Correspondence and requests for material should be addressed to H.R.B.

[#]bourne@cmp.ucsf.edu

Note added in proof: The data concerning the concentrations of PI(3)K inhibitors required to block Akt phosphorylation are included in the accompanying manuscript by Wang *et al.* *Nature Cell Biol.*

Supplementary Information is available on *Nature Cell Biology's* website (<http://cellbio.nature.com>).

Competing Financial Interests: The authors declare that they have no competing financial interests.

PtdInsP₃ production interfere with cell polarity and chemotaxis in many systems^{5–10}. Furthermore, PtdInsP₃ itself suffices to induce cell polarity and motility in neutrophils¹¹ and fibroblasts¹². Thus, PtdInsP₃ occupies a privileged position as the most upstream molecule known to exhibit asymmetry during chemotaxis and one of the most downstream molecules that suffices to induce cell polarity and motility. To explore how this lipid regulates cell polarity, we have assessed the effects of delivering exogenous PtdInsP₃ to cells which contain an internal probe that allows the spatial distribution of PI(3)K lipid products to be determined.

PtdInsP₃ polarization during chemotaxis could result from the polarized activation of chemoattractant receptors or PI(3)Ks. Alternatively, it could reflect signals generated downstream of PtdInsP₃ production. To test the latter hypothesis, we sought to deliver exogenous PtdInsP₃ to neutrophils. PtdInsP₃ and other anionic phospholipids do not permeate the membranes of most cells. However, when complexed to cationic carriers, such as histone, phosphoinositides can be delivered to cells and exert physiological responses¹³. To assess the spatial distribution of PI(3)K lipid products, we used neutrophil-like differentiated HL-60 cells, which express PH-Akt-GFP (the pleckstrin homology domain of Akt tagged with green fluorescent protein), a fusion protein that specifically binds to PtdInsP₃ and PtdIns(3,4)P₂ (ref. 3). At early times (30–120 s) after incubation with C16-PtdInsP₃ (30 μM) complexed to histone (10 μM), cells exhibit ruffling and uniform translocation of PH-Akt-GFP to the plasma membrane (Figs 1a–d and 2b; 27 out of 59 cells translocated PH-Akt-GFP between 30 and 60 s). Lower concentrations of C16-PtdInsP₃ (10 μM) complexed to histone (3 μM) elicited approximately half this response (16 out of 74 cells translocated PH-Akt-GFP between 30 and 60 s).

Cells polarize after incubation with PtdInsP₃-histone for 2–3 min. Surprisingly, they also asymmetrically accumulate PH-Akt-GFP at the leading edge (Fig. 1e,f, arrowheads; also see Fig. 2c; 15 out of 55 cells showed polarized PH-Akt-GFP in this time frame) and migrate 1–2 cell diameters. These translocations can be observed most easily in the surface plots of Fig. 2. Polarity was usually maintained for 2–10 min. For almost all of the cells, the pattern of PH-Akt-GFP recruitment and polarization mirrored their actin rearrangements with the final polarized morphology, ranging from a more fibroblast-like crescent to the polarized cell pictured in Fig. 2e,f; the latter pattern is typical of the majority of polarized cells. The patterns of polarity closely resemble those seen with fMLP as the stimulus. Similar data was obtained using a PtdInsP₃ antibody (see Supplementary Information, Fig. S1). These data suggest that PtdInsP₃ can induce its own asymmetry. Unstimulated cells (Figs 1g and 2a) and cells incubated with PtdInsP₃ without a histone carrier (Fig. 1h) failed to induce translocation of PH-Akt-GFP. This suggests that the PtdInsP₃-histone effect is not mediated by an extracellular PtdInsP₃ receptor (2 out of 66 unstimulated cells and 2 out 58 cells stimulated with PtdInsP₃ alone translocated PH-Akt-GFP uniformly at 30–60 s; 0 out of 63 unstimulated cells and 0 out of 67 cells stimulated with PtdInsP₃ alone exhibited polarized PH-Akt-GFP recruitment at 2–3 min). This effect was not a general property of lipid-histone complexes, as PtdIns(4,5)P₂-histone failed to induce recruitment of PH-Akt-GFP (Fig. 1i; 5 out of 52 cells uniformly translocated PH-Akt-GFP in 30–60 sec, and 0 out of 56 cells exhibited polarized PH-Akt-GFP recruitment at 2–3 min). A GFP-tagged chemoattractant receptor¹⁴ remained uniformly distributed throughout the plasma membrane in polarized cells, as previously described for neutrophils¹⁴ and *Dictyostelium*¹⁵. This suggests that the PH-Akt-GFP asymmetry we observed after PtdInsP₃-histone stimulation is not a reflection of cell morphology (Fig. 2d). It is important to note that translocation of PH-Akt-GFP and polarization in response to PtdInsP₃-histone is less robust than that seen in response to an optimal dose of chemoattractant. This suggests that activated receptors stimulate production of more PtdInsP₃ than we are able to deliver to the cells exogenously,

or that signalling from chemoattractant receptors provides signals to the cell polarization process in addition to PtdInsP₃.

To determine whether endogenous signalling cascades are necessary for the effects of PtdInsP₃-histone on cells, we analysed the consequences of inhibiting endogenous PI(3)Ks and Rho GTPases with a PI(3)K inhibitor (LY 294002) or *Clostridium difficile* toxin B (toxB), which inhibits the actions of Rac, Rho and Cdc42 GTPases. Pretreating cells with LY 294002 (200 μM for 20 min) completely prevented PtdInsP₃-histone from inducing PH-Akt-GFP translocation (Fig. 3a; 0 out of 89 cells responded by translocating PH-Akt-GFP). Wortmannin (200 nM) produces similar effects (data not shown). Approximately 70% inhibition was observed with 100 μM LY 294002 (10 out of 67 cells responded with PH-Akt-GFP translocation (data not shown)). Similar data was obtained using a PtdInsP₃ antibody instead of PH-Akt-GFP (see Supplementary Information, Fig. S1). These results suggest that the PH-Akt-GFP translocation observed after exposure of cells to PtdInsP₃-histone does not depend solely on exogenous PtdInsP₃, but rather that PtdInsP₃ cooperates with endogenous PI(3)Ks in a positive feedback loop that is necessary to generate enough PtdInsP₃ for a response. Although our data are most consistent with a positive feedback loop, we cannot rule out a purely permissive role for endogenous PI(3)K or basal PtdInsP₃ levels in the effects of exogenous PtdInsP₃-histone with these experiments. The concentrations of LY294002 and wortmannin needed to block PtdInsP₃-induced PH-Akt-GFP translocation are high when compared to doses of these inhibitors needed to block PI(3)K signalling in other cells, such as fibroblasts. However, these mirror the concentrations necessary to block Akt phosphorylation (see Note added in proof), PH-Akt-GFP translocation³ and PtdInsP₃ antibody staining (F. Wang, personal communication) in HL-60 cells in response to chemoattractant stimulation. This suggests that these cells are relatively resistant to PI(3)K inhibitors. Intriguingly, at later times (greater than 5 min), some LY 294002-treated cells do show uniform translocation of PH-Akt-GFP to the plasma membrane (17 out of 122 cells exhibited this behaviour (data not shown)). This suggests that, given time, enough PtdInsP₃ can be delivered to the cells to generate PH-Akt-GFP translocation, even without a contribution from endogenous PI(3)Ks. However, these cells consistently failed to develop polarized PH-Akt-GFP distributions, (1 out of 17 cells showing translocation went on to polarize PH-Akt-GFP), suggesting that the PtdInsP₃ positive feedback loop is important for developing PtdInsP₃ polarity.

Similarly, pretreating cells with toxB prevented PtdInsP₃-histone from inducing PH-Akt-GFP translocation (Fig. 3b). Because toxB also can induce cell lethality, we tested for cell viability by subsequently treating cells with insulin, which we previously demonstrated to induce Rho-GTPase-independent translocation of PH-Akt-GFP to the plasma membrane³. Only cells that translocated PH-Akt-GFP in response to insulin (Fig. 3c) were scored for their previous responsiveness to PtdInsP₃-histone; of 77 cells that exhibited PH-Akt-GFP translocation in response to insulin, none showed PH-Akt-GFP translocation in response to incubation with PtdInsP₃-histone. These data suggest that one or more Rho GTPases are necessary components of the PtdInsP₃-histone-induced PtdInsP₃ positive feedback loop. Rho GTPase inhibition also blocks PH-Akt-GFP translocation³ and Akt activation (G. Servant and D. Stokoe, personal communication) in cells responding to chemoattractant, suggesting that a similar signalling cascade operates during chemotaxis.

The inhibitory effects of LY 294002 and toxB on responses to exogenous PtdInsP₃-histone treatment could result from inhibition of PtdInsP₃ delivery to the cells, rather than from inhibiting cooperation between exogenous PtdInsP₃ and endogenous signalling cascades. To discriminate between these possibilities, we analysed delivery of fluorescently derivatized NBD-PtdInsP₃-unlabelled histone to cells with and without inhibitors of PI(3)K and Rho GTPases. In control cells that failed to polarize, NBD-PtdInsP₃-histone was distributed

uniformly at the cell periphery (Fig. 4a, arrowhead). By contrast, in cells that did polarize, NBD-PtdInsP₃ accumulated in the cell posterior (Fig. 4a, arrow). An important qualification of these results is that the fluorescent probe, located at the end of one of the phospholipid's fatty acid tails, is not destroyed by metabolism of the inositol head-group. Consequently, the observed fluorescence reflects delivery of exogenous PtdInsP₃-histone to the cells, although it probably does not solely represent unmodified PtdInsP₃. Indeed, we never observe preferential accumulation of the PH-Akt-GFP at the trailing edge of polarized cells. Thus the NBD-PtdInsP₃ results suggest that accumulation of PH-Akt-GFP at the leading edge of polarized cells does not represent accumulation of exogenous PtdInsP₃-histone at this location. Delivery of NBD-PtdInsP₃ to the cell periphery depends on the presence of histones (Fig. 4b). Although treatment with LY 294002 (Fig. 4c) or toxB (Fig. 4d) prevents cell polarization, these agents do not inhibit delivery of exogenous NBD-PtdInsP₃ to the cell periphery. Taken together, the data suggest that these agents do not produce their effects by inhibiting the cellular uptake of PtdInsP₃-histone.

Discussion

These results, showing that translocation of PH-Akt-GFP to the plasma membrane in response to PtdInsP₃-histone requires endogenous PI(3)K activity and Rho GTPases, can be explained by postulating a positive feedback loop that involves PtdInsP₃ and the Rho GTPases. Such a feedback loop could explain paradoxical epistatic relations between Rho GTPases and PI(3)Ks identified in genetic, pharmacological and biochemical analyses: PI(3)K activity has been shown to function upstream of Rac and Cdc42 activation^{16,17}, but Rac and Cdc42 have been shown to function upstream of PtdInsP₃ generation^{14,18–21}; this apparent paradox has sometimes been observed in the same cell, for example, in neutrophils^{14,17} and T-cells¹⁹. Our findings suggest that these conflicting results may be explained by PtdInsP₃ and Rho GTPases functioning both upstream and downstream of one another in a positive feedback loop.

One question concerns how such a feedback loop contributes to cell polarity during chemotaxis. A possible clue comes from models of mechanisms by which developmental organizers form self-organizing patterns from small gradients or stochastic differences in signalling²². The first postulated ingredient of such pattern formation systems is a signal that amplifies itself in a short-range positive feedback fashion. We propose that the PtdInsP₃- and Rho GTPase-dependent positive feedback loop provides this function in eukaryotic chemotaxis. The second ingredient of this self-organizing pattern formation system²² is that signals from the activator generate a more long-range inhibitor of signalling. Good candidates for this inhibitory function in eukaryotic chemotaxis include negative regulators of PtdInsP₃ accumulation, such as the lipid phosphatases PTEN (phosphatase and tensin homologue deleted on chromosome ten)^{23,24} and SHIP (SH2-containing inositol phosphatase)²⁵, and negative regulators of Rho GTPase activation (for example, a recently identified negative feedback loop in *Saccharomyces cerevisiae*, in which Cdc42 induces phosphorylation and inactivation of its own guanine nucleotide exchange factor²⁶). In addition to chemotaxis²², pattern formation systems that are consistent with this general model (though not necessarily the same components) include hydra regeneration and retinotectal mapping. Good candidates for components in the positive feedback loop include: PtdInsP₃ activation of guanine nucleotide exchange factors for Rac, such as Prex²⁷, Cdc42/Rac-induced activation of PtdInsP₃ production through direct binding to the Rho GAP domain of the PI(3)K adapter p85 (refs 20,21,28) or induction of PI(4,5)P₂ generation through recruitment of PI(5)K²⁹, which could increase availability of substrate for PtdInsP₃ production by PI(3)Ks.

In summary, PtdInsP₃ asymmetries are observed during chemotaxis of many cells, from neutrophils³ to *Dictyostelium*^{1,2} to fibroblasts⁴, and in response to very different stimuli, such as ligands for G-protein coupled receptors^{1–3} and tyrosine kinase receptors⁴, as well as direct delivery of PtdInsP₃, as we have shown. We propose that the emergent properties of positive and negative regulatory links between PtdInsP₃ and Rho GTPases constitute a broadly conserved module for establishing cell polarity during eukaryotic chemotaxis. Such a polarity module could account for the remarkable convergence of behaviour among these widely diverse cells and chemotactic stimuli. Important future directions include dissecting the wiring of the putative positive and negative feedback loops and developing better tools to spatially analyse and manipulate protein and lipid activities. This will allow us to gain a deeper understanding of how eukaryotic cells polarize and migrate in response to cues from the world around them.

Methods

Cell preparation

HL-60 cells expressing PH-Akt-GFP³ were stimulated to differentiate, as described³, except that endotoxin-free hybridoma-tested dimethyl sulphoxide (D2650; Sigma, St Louis, MO) was used. Treatment with LY 294002 and toxB were performed as described³, except that LY 294002 was continuously incubated with the cells for LY 294002 treatment.

Lipid delivery

Long chain (Di-C₁₆) synthetic phospholipids (Echelon, Salt Lake City, UT) were freshly prepared at 300 μM in 150 mM sodium chloride, 4 mM potassium chloride and 20 mM Hepes at pH 7.2, and resuspended by bath sonication or vigorous vortexing. Histone-phospholipid complexes were prepared by incubating 300 μM phospholipids with 100 μM freshly prepared histone (Echelon), vortexed vigorously, incubated for 5 min at room temperature and diluted 1:10 with modified Hanks buffered saline solution³⁰ immediately before addition to HL-60 cells in suspension. Cells were immediately added to an agarose-lined coverslip using wide-bore pipette tips³⁰.

Microscopy

Images were acquired with an epifluorescence microscope (Nikon, Melville, NY) and an axiovert confocal microscope (Zeiss, Woburn, MA). Quantitation of PH-Akt-GFP translocation and cell polarization were performed on random fields of living cells for a minimum of 3 independent experiments. We defined polarization as Akt recruitment continuously covering 25–75% of the cell surface. Cells with two independent fronts were not counted as polarized. Surface plots for Fig. 2 were generated from confocal images using NIH Image1.62.

Supplementary Material

Refer to Web version on PubMed Central for supplementary material.

Acknowledgments

We thank S. Ozaki and J. Chen for NBD-PtdInsP₃ synthesis, C. Kelley and M. Warny for the kind gift of *Clostridium difficile* toxin B, R. Tsien's lab for the PtdInsP₃-AM used in early experiments, V. Niggli for advice on using this compound with neutrophils, F. Wang for protocols for the PtdInsP₃ antibody, Echelon for the gift of phospholipids and histones, and C. Bargmann, C. Carpenter and C. Kenyon for helpful discussions. This work was in part supported by grants from the National Institutes of Health to H.R.B., L.C.C. (GM41890), M.W.K. (GM26825), P.O.N. (GM62734-03), and G.D.P. (NS29632).

O.D.W. was supported by a Howard Hughes Medical Institute predoctoral fellowship and the Damon Runyon Cancer Research Fund.

References

1. Meili R, et al. *EMBO J* 1999;18:2092–2105. [PubMed: 10205164]
2. Jin T, Zhang N, Long Y, Parent CA, Devreotes PN. *Science* 2000;287:1034–1036. [PubMed: 10669414]
3. Servant G, et al. *Science* 2000;287:1037–1040. [PubMed: 10669415]
4. Haugh JM, Codazzi F, Teruel M, Meyer T. *J Cell Biol* 2000;151:1269–1280. [PubMed: 11121441]
5. Niggli V, Keller H. *Eur J Pharmacol* 1997;335:43–52. [PubMed: 9371545]
6. Vanhaesebroeck B, et al. *Nature Cell Biol* 1999;1:69–71. [PubMed: 10559867]
7. Funamoto S, Milan K, Meili R, Firtel RA. *J Cell Biol* 2001;153:795–810. [PubMed: 11352940]
8. Hirsch E, et al. *Science* 2000;287:1049–1053. [PubMed: 10669418]
9. Li Z, et al. *Science* 2000;287:1046–1049. [PubMed: 10669417]
10. Sasaki T, et al. *Science* 2000;287:1040–1046. [PubMed: 10669416]
11. Niggli V. *FEBS Lett* 2000;473:217–221. [PubMed: 10812078]
12. Derman MP, et al. *J Biol Chem* 1997;272:6465–6470. [PubMed: 9045671]
13. Ozaki S, DeWald DB, Shope JC, Chen J, Prestwich GD. *Proc Natl Acad Sci USA* 2000;97:11286–11291. [PubMed: 11005844]
14. Servant G, Weiner OD, Neptune ER, Sedat JW, Bourne HR. *Mol Biol Cell* 1999;10:1163–1178. [PubMed: 10198064]
15. Xiao Z, Zhang N, Murphy DB, Devreotes PN. *J Cell Biol* 1997;139:365–374. [PubMed: 9334341]
16. Hawkins PT, et al. *Curr Biol* 1995;5:393–403. [PubMed: 7627555]
17. Benard V, Bohl BP, Bokoch GM. *J Biol Chem* 1999;274:13198–13204. [PubMed: 10224076]
18. Yang FC, et al. *Immunity* 2000;12:557–568. [PubMed: 10843388]
19. Genot EM, et al. *Mol Cell Biol* 2000;20:5469–5478. [PubMed: 10891487]
20. Zheng Y, Bagrodia S, Cerione RA. *J Biol Chem* 1994;269:18727–18730. [PubMed: 8034624]
21. Bokoch GM, Vlahos CJ, Wang Y, Knaus UG, Traynor-Kaplan AE. *Biochem J* 1996;315:775–779. [PubMed: 8645157]
22. Meinhardt H, Gierer A. *Bioessays* 2000;22:753–760. [PubMed: 10918306]
23. Liliental J, et al. *Curr Biol* 2000;10:401–404. [PubMed: 10753747]
24. Stambolic V, et al. *Cell* 1998;95:29–39. [PubMed: 9778245]
25. Liu Q, et al. *Genes Dev* 1999;13:786–791. [PubMed: 10197978]
26. Gulli M, et al. *Mol Cell* 2000;6:1155–1167. [PubMed: 11106754]
27. Welch HCE, et al. *Cell* 2002;108:809–821. [PubMed: 11955434]
28. Toliás KF, Cantley LC, Carpenter CL. *J Biol Chem* 1995;270:17656–17659. [PubMed: 7629060]
29. Carpenter CL, Toliás KF, Couvillon AC, Hartwig JH. *Adv Enzyme Regul* 1997;37:377–390. [PubMed: 9381982]
30. Weiner OD, et al. *Nature Cell Biol* 1999;1:75–81. [PubMed: 10559877]

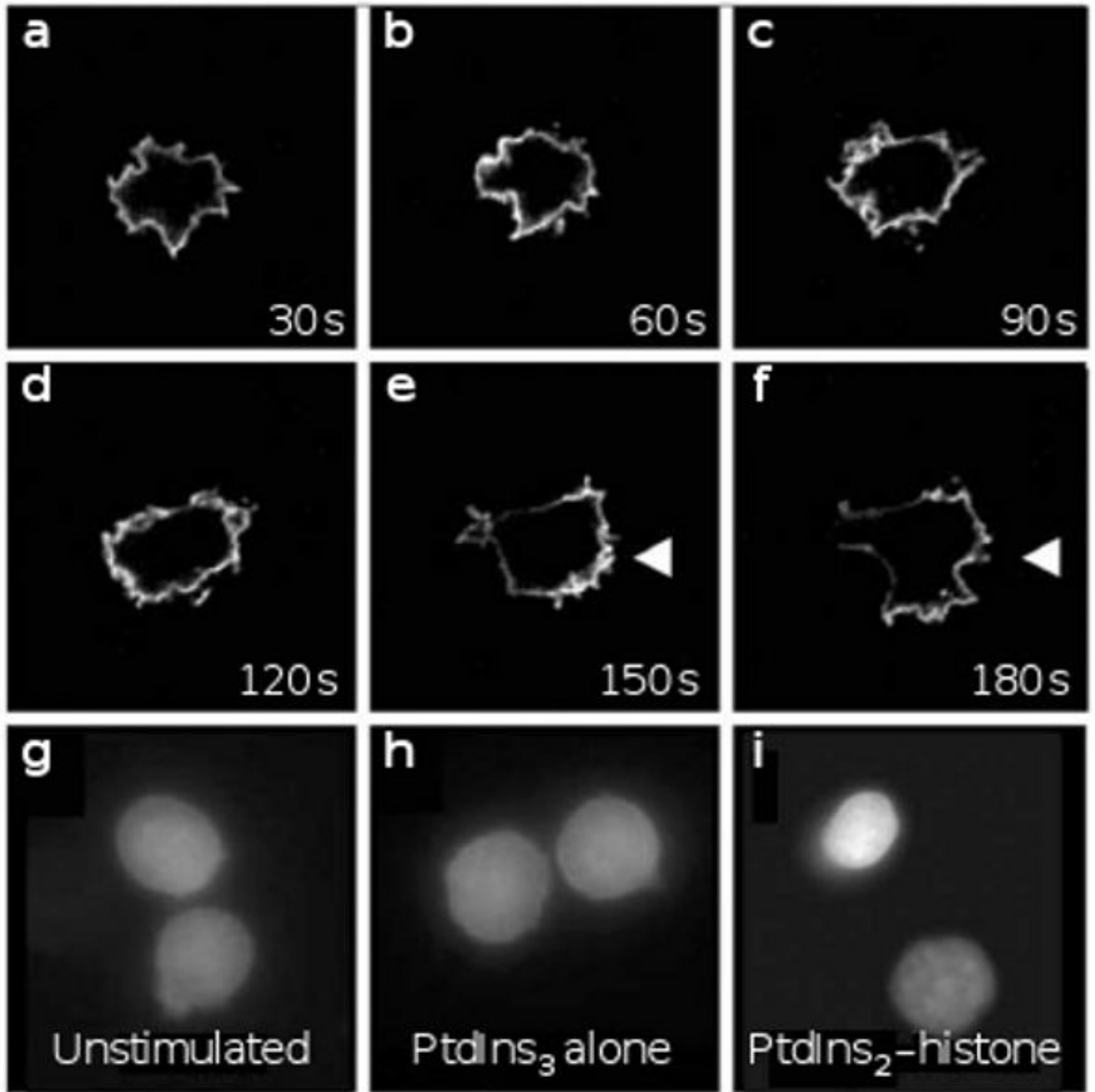


Figure 1. PtdInsP₃–histone induces translocation of PH-Akt–GFP

A spatial readout is shown for generation of PtdInsP₃ and PtdIns(3,4)P₂ at the plasma membrane in neutrophil-differentiated HL-60 cells. **a–f**, Time course of cells exposed to PtdInsP₃ (30 μM)–histone (10 μM). **g**, Unstimulated cells. **h**, Cells exposed to PtdInsP₃ (30 μM) without histone carrier. **i**, Cells exposed to PtdIns(4,5)P₂ (30 μM)–histone (10 μM).

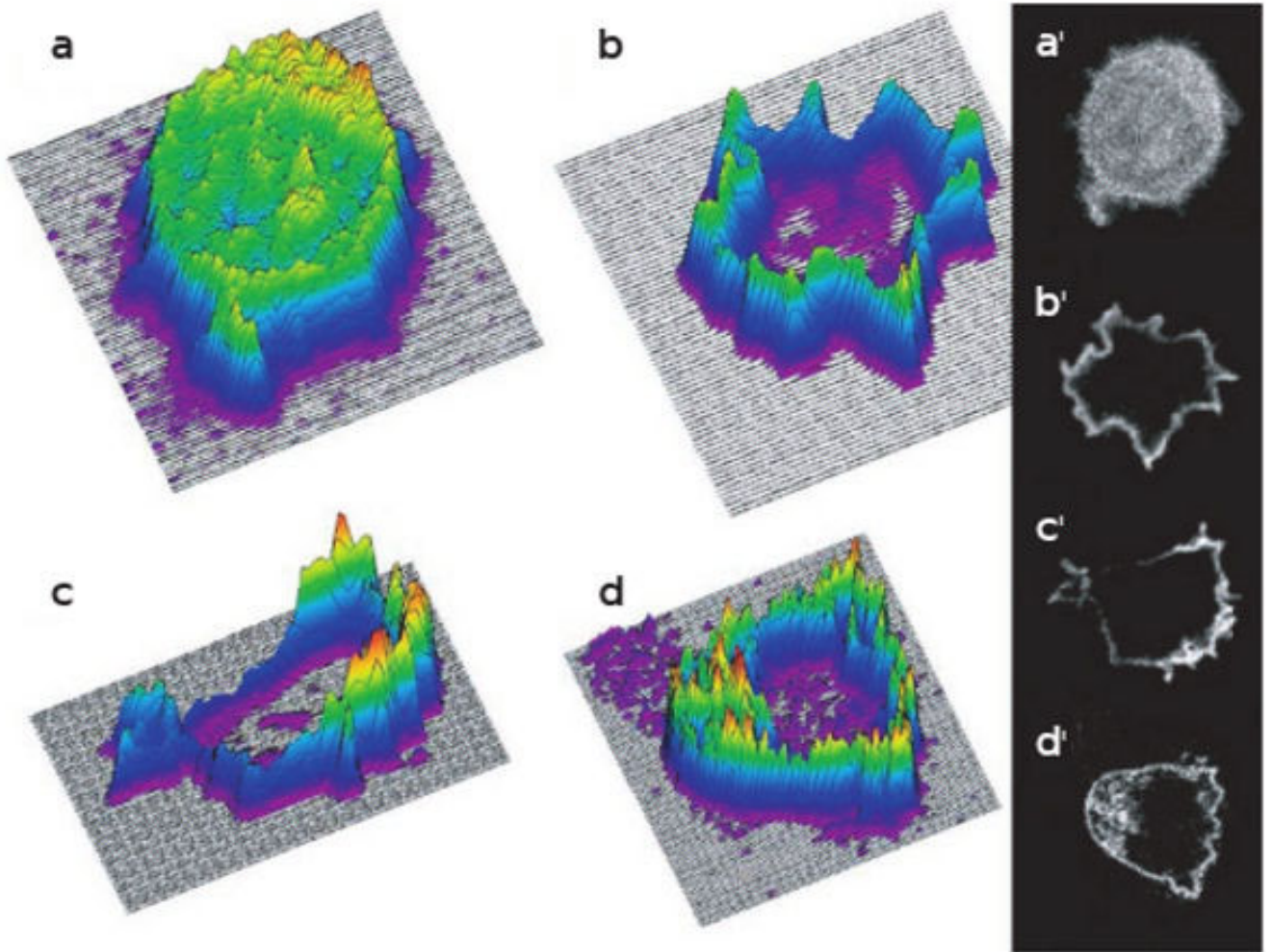


Figure 2. Surface plots of PH-Akt-GFP distribution in neutrophil-differentiated HL-60 cells
 Height corresponds to fluorescence intensity of each pixel from confocal images of cells. **a**, An unstimulated cell. **b**, A cell stimulated with PtdInsP₃-histone for 30 s. **c**, A cell stimulated with PtdInsP₃-histone for 150 s. **d**, A cell expressing the chemokine receptor C5AR-GFP¹⁴ stimulated with 100 nM FMLP for 150 s. **a'-d'**, Confocal images from which the surface plots in **a-d** were generated.

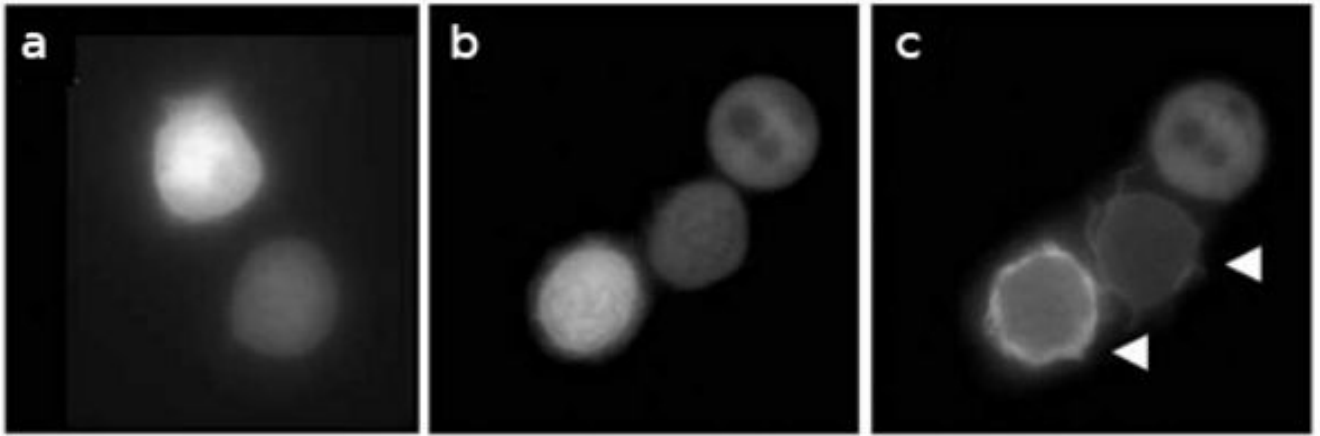


Figure 3. PI(3)K and Rho GTPase inhibitors block PtdInsP₃–histone-induced PH-Akt–GFP translocation

a, Cells treated with LY 294002 (200 μ M) for 20 min and then stimulated with PtdInsP₃ (30 μ M)–histone (10 μ M). Similar doses of LY 294002 were needed to block phosphorylation of Akt in response to chemoattractant (see Supplementary Information, Fig. S2). **b,c**, Cells pretreated with *Clostridium difficile* toxin B (90 μ g ml⁻¹) for 4–5 h and sequentially stimulated with PtdInsP₃–histone (**b**) and then insulin (**c**) to test for cell viability. In **c**, two of the three cells are viable, as judged by PH-Akt–GFP translocation in response to insulin (arrowheads)

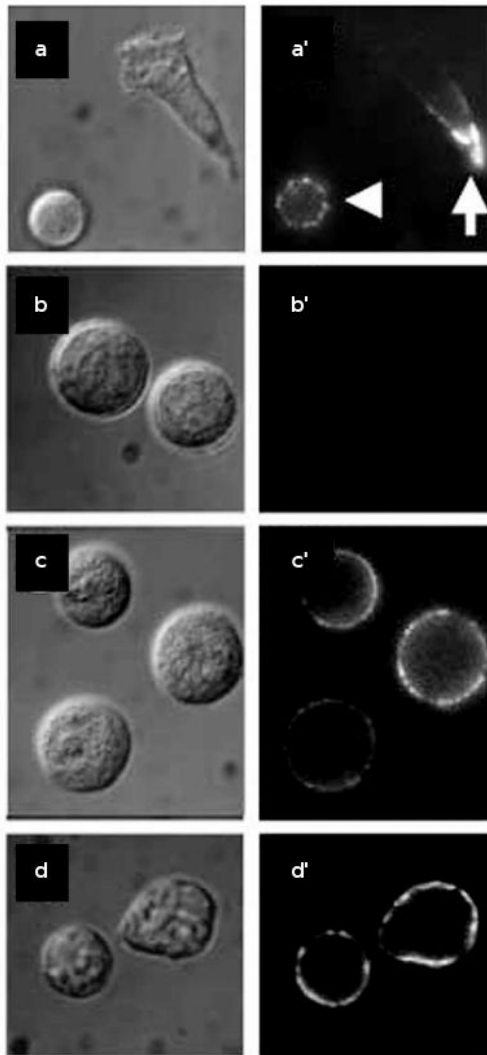


Figure 4. Endogenous PI(3)K and Rho GTPases are not required for PtdInsP₃-histone uptake
a, Control cells treated with fluorescent NBD-PtdInsP₃ (30 μM)-histone (10 μM) for 5 min.
b, Cells treated with NBD-PtdInsP₃ (30 μM) without histone carrier. **c**, Cells pretreated with LY 294002 (200 μM) for 20 min and then exposed to NBD-PtdInsP₃ (30 μM)-histone (10 μM). **d**, Cells were pretreated with toxB and then exposed to NBD-PtdInsP₃ (30 μM)-histone (10 μM). **a-d**, Nomarski images, **a'-d'**, immunofluorescence images.